DISCLAIMER

This report was prepared as an account of work sponsored by an agency of the United States Government. Neither the United States Government nor any agency thereof, nor any of their employees, makes any warranty, express or implied, or assumes any legal liability or responsibility for the accuracy, completeness, or usefulness of any information, apparatus, product, or process disclosed, or represents that its use would not infringe privately owned rights. Reference herein to any specific commercial product, process, or service by trade name, trademark, manufacturer, or otherwise does not necessarily constitute or imply its endorsement, recommendation, or favoring by the United States Government or any agency thereof. The views and opinions of authors expressed herein do not necessarily state or reflect those of the United States Government or any agency thereof. Reference herein to any social initiative (including but not limited to Diversity, Equity, and Inclusion (DEI); Community Benefits Plans (CBP); Justice 40; etc.) is made by the Author independent of any current requirement by the United States Government and does not constitute or imply endorsement, recommendation, or support by the United States Government or any agency thereof.

INL/RPT-25-89342-Revision-0

M3AS-25IN1002073: Analysis of data from irradiation testing of printed strain gauges in prototypic nuclear environments

December 2025

Timothy Le Phero, Bibo Zhong, Michael D McMurtrey, Joshua E Daw, Amey Rajendra Khanolkar, Md Omarsany Bappy, Yanliang Zhang, Brian J. Jaques

Changing the World's Energy Future

Idaho National Laboratory

INL is a U.S. Department of Energy National Laboratory operated by Battelle Energy Alliance, LLC

INL/RPT-25-89342-Revision-0

M3AS-25IN1002073: Analysis of data from irradiation testing of printed strain gauges in prototypic nuclear environments

Timothy Le Phero, Bibo Zhong, Michael D McMurtrey, Joshua E Daw, Amey Rajendra Khanolkar, Md Omarsany Bappy, Yanliang Zhang, Brian J. Jaques

December 2025

Idaho National Laboratory
Idaho Falls, Idaho 83415

http://www.inl.gov

Prepared for the
U.S. Department of Energy
Under DOE Idaho Operations Office
Contract DE-AC07-05ID14517

[INL/RPT-XX-XXXXX]
[Revision X] [only after initial release]

M3AS-25IN1002073: Analysis of data from irradiation testing of printed strain gauges in prototypic nuclear environments

Advanced Sensors and Instrumentation (ASI)

ASI Milestone Report

DECEMBER 2025

Timothy L. Phero
Amey R. Khanolkar
Bibo Zhong
Joshua Daw

Idaho National Laboratory

Md Omarsany Bappy
Yanliang Zhang

University of Notre Dame

Brian J. Jaques

Boise State University

Idaho National Laboratory

[INL/RPT-XX-XXXXX
[Revision X] [only after initial release]

M3AS-25IN1002073: Analysis of data from irradiation testing of printed strain gauges in prototypic nuclear environments

ASI Milestone Report

Timothy L. Phero
Amey R. Khanolkar
Bibo Zhong
Joshua Daw
Idaho National Laboratory
Md Omarsany Bappy
Yanliang Zhang
University of Notre Dame
Brian J. Jaques
Boise State University

December 2025

Idaho National Laboratory
Idaho Falls, Idaho 83415

http://www.inl.gov

Prepared for the
U.S. Department of Energy
Office of Nuclear Energy
Under DOE Idaho Operations Office
Contract DE-AC07-05ID14517

Page intentionally left blank

ABSTRACT

Advancement in additively manufactured strain gauges help address critical technology gaps to accurately monitor real-time materials behavior in reactor experiments. This is critical as it provides data to inform predictive models and simulations that enhance the development of reactors and fuel cycle systems. In this report, additively manufactured strain gauges are exposed to a neutron irradiation environment at the Ohio State University Research Reactor. This report goes over a 2-week campaign for neutron irradiating printed resistive strain gauges and capacitive strain gauges. These results complement the prior separate effects (i.e., mechanical strain, temperature, etc.) testing that were performed on these additive manufactured sensors and presented in prior milestone reports. These results also help progress our understanding of their usage in harsh environment applications. The outcome of developing advanced sensing and instrumentation capabilities plays an important role in increasing the safety, reliability, and energy efficiency of both next-generation and existing nuclear reactors.

Page intentionally left blank

ACKNOWLEDGMENTS

This work was supported by the Department of Energy Advanced Sensors and Instrumentation program under DOE Idaho Operations Office Contract DE-AC07-05ID14517. This work also was supported by the Nuclear Science User Facilities (NSUF) Rapid Turnaround Experiment (RTE) award (award number: 24-4969) under DOE Idaho Operations Office Contract DE-AC07- 051D14517 as part of a Nuclear Science User Facilities Experiments. We would also like to thank the Ohio State University Research Reactor staff: Kevin Herminghuysen, Susan White, Joel Hatch, Leanne Wegley, and Andrew Kauffman for their advice and support for the successful irradiation campaign.

Page intentionally left blank

CONTENTS

FIGURES

TABLES

Page intentionally left blank

ACRONYMS

AM	Additive Manufacturing
CSG	Capacitive Strain Gauge
CTE	Coefficient of Thermal Expansion
DAQ	Data Acquisition
MTR	Materials Test Reactor
OSURR	Ohio State University Research Reactor
PIE	Post Irradiation Examination
RSG	Resistive Strain Gauge

Page intentionally left blank

Analysis of Data from Irradiation Testing of Printed Strain Gauges in Prototypic Nuclear Environments

1. INTRODUCTION

The development of novel sensors that are resilient to harsh environments have an important role in increasing the safety, reliability, and energy efficiency of both next-generation and existing nuclear reactors. Although sensors have the potential to positively impact the future of sustainable energy production, the harsh operating conditions in the core of a nuclear reactor and confined spacing between the fuels and cladding in nuclear reactors make it a challenge to obtain accurate and reliable sensing performance. To address these limitations, there are efforts to develop in-pile instrumentation that enable the miniaturization of current sensing technologies reduce the invasiveness and enable their application when collecting in-pile measurements [1, 2]. The use of additive manufacturing (AM) as a fabrication technique is of interest for developing in-pile devices as it allows for the direct deposition of material onto a substrate including curved surfaces (Figure 1). AM technologies, including aerosol jet printing [2] and ink-jet printing [3], are of interest for fabricating sensors since they can print high resolution electronics at a moderately low cost [3], while also enabling the deposition of materials with tailored composition and chemistry. The integration of AM sensors and instrumentation technologies on nuclear relevant materials will address critical technology gaps to accurately monitor materials behavior and provide data to inform predictive models and simulations to enhance the development of reactors and fuel cycle systems.

Figure 1. Conformal printing on a 16 mm diameter Haynes 244 tube

AM printed sensors have an advantage over current wire and foil sensors because of their small form factor when embedded into the operating conditions of nuclear reactors. As presented in the prior reports [4], printing process parameters, as well as ink formulation and substrate material affect the mechanical and electrical behavior of the printed sensors. The manufacturing flexibility of the AM printed sensors provides opportunities to develop a sensor with materials properties favorable for harsh environment sensing applications. A challenge in realizing the potential for harsh environmental sensing is the limited understanding of inks that are formulated with and printed on nuclear relevant materials. In addition, there is a limited understanding of the effects of neutron irradiation and conformal printing on the reliability of AM printed sensors. Such information will provide valuable information on the sensor's performance and duration of operation in a reactor. Although previous work have looked at the separate effects of elevated temperature on the performance of AM printed resistive strain gauges [2] and capacitive strain gauges [5], there is no work, as far as the authors are aware, that look at the effects of neutron irradiation on these printed strain gauges. This milestone reports help fulfill this need by investigating the separate effects of neutron and gamma irradiation on the performance of AM resistive strain gauges (RSG) and capacitive strain gauges (CSG) deployed in a materials test reactor (MTR). These tests are performed at the Ohio State University Research Reactor (OSURR), a 450 kW MTR that allows for instrumented experiments and real-time monitoring at various steady-state reactor powers and power transients [6].

2. EXPERIMENTAL PROCEDURE

2.1. OSURR Irradiation

The OSURR is a pool-type materials test reactor that has multiple beam ports and dry tubes that can operate up to a maximum reactor power of 450 kW. The printed sensors are inserted and mounted on the furnace (Figure 3a) so that the printed sensors are securely lowered in the dry-tube (Figure 3). The irradiation test at OSURR was broken into two 1-week campaigns. The reactor power, temperature, and neutron fluence at the peak neutron flux zone (Figure 4) are shown in Figure 2 for each of the two campaigns.

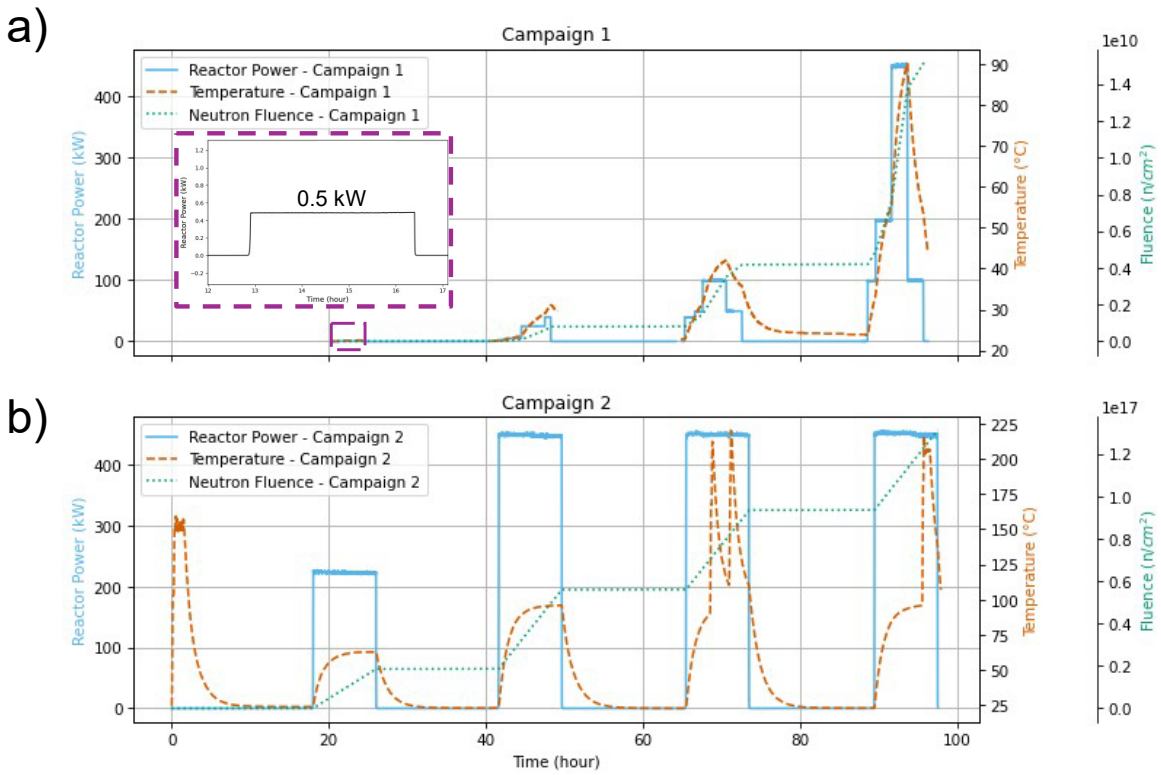

Figure 2. Reactor power, temperature, neutron fluence at peak position (i.e., 9.5" above spacer in furnace as shown in Figure 4) for a) campaign 1 and b) campaign 2.

2.1.1. Campaign 1

At approximately 9.5” above the aluminum spacer in the furnace (Figure 4), the total expected neutron flux was measured to be 1.1×10^{12} n/cm^2/s. These tests were conducted in an ambient environment with no external heating from the furnace. Even though the furnace was not used for heating for this initial campaign, the gamma radiation in a reactor allowed for the sample to heat up giving a gamma-heating effect. The gamma dose rate in silicon (Si) while using the 9.5” dry tube is 4.4×10^6 rad-Si/hr at the maximum reactor power (i.e., 450 kW). To measure this change in temperature of the samples due to gamma heating, a type-k thermocouple is instrumented on the backside of the samples. These temperature rises can affect the performance of the printed sensors. Figure 2 shows the reactor powers that were used during the four-day test of the strain gauge.

Table 1 tabulates the reactor power and hold duration at the reactor power across the four days of testing in this 1st campaign.

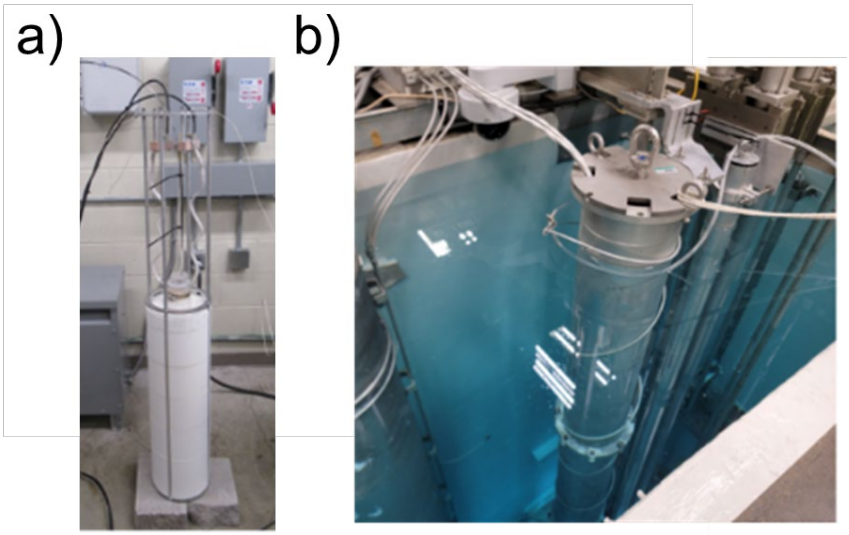

Figure 3. a) The silicon carbide furnace used to mount the sample and lowered in the b) 9.5" dry tube at the OSU research reactor

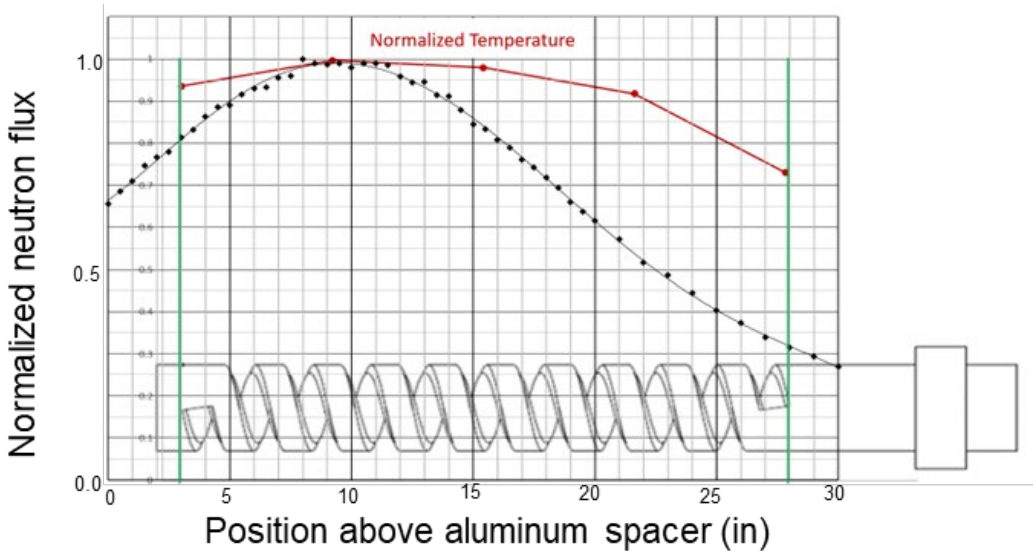

Figure 4. The expected neutron flux profile within the 9.5" dry tube used in the OSU research reactor

Table 1. Reactor power for all four days of testing at OSURR for Campaign 1. This is visually represented in Figure 2.

Test day	Power (kW)	Hold duration (hr)
Day 1	0.5	3.5
Day 2	0.5	0.5
	2.5	1
	5	2
	25	3
	40	0.75
Day 3	40	1.25
	50	1
	100	3
	50	2
Day 4	100	1
	200	2
	450	2
	100	2

2.1.2. Campaign 2

For the 2nd campaign, the samples were also put in a fixture so that the sensing region of the strain gauge was 9.5" above the aluminum spacer in the furnace (Figure 4). The total expected neutron flux in this region of the furnace during the 2nd campaign was measured to be 1.3×10^{12} n/cm^2/s. These tests were conducted in an ambient environment on Day 2 and Day 3. However, on days 1, 4, and 5, the furnace was turned on to include external heating. The gamma dose rate in silicon while using the 9.5" dry tube is 4.5×10^6 rad-Si/hr at the maximum reactor power. To measure this change in temperature of the samples due to gamma heating, a type-k thermocouple is instrumented on the backside of the samples. These temperature rises can affect the performance of the printed sensors. Table 2 tabulates the reactor power and holds duration at the reactor power across the four 8-hour days of irradiation during this 2nd campaign.

Table 2. Reactor power for all four days of testing at OSURR for campaign 2. This is visually represented in Figure 2b.

Test day	Power (kW)	Reactor Power hold duration (hr)	Furnace Temperature (°C)	Furnace hold duration (min)
Day 1	0	0	150	60
Day 2	225	8	0	0
Day 3	450	8	0	0
Day 4	450	3	0	0
	450	2.5	215	1
	450	2.5	215	1
Day 5	450	6.5	0	0
	450	1	215	60
	450	0.5	0	0

2.2. Data Acquisition

2.2.1. Campaign 1

The RSGs are measured using a Wheatstone bridge circuit in a half-bridge configuration. A NI-PXIe-4330 strain bridge module was integrated into a NI-PXIe 1071 chassis and a LabVIEW program that was used for data acquisition. Prior to measurement, an offset and shunt calibration was performed on the strain gauge to correct for any resistance errors stemming from the lead wires and individual resistors within the bridge. A bridge excitation of 2.0 V was used during the measurement. CSG was measured using a precision LCR-meter (Agilent E4980a) using a four-point measuring technique with kelvin clip leads (16089C, Keysight). A standard short and open correction was performed to remove parasitic capacitance from the environment and LCR to mitigate any errors from the CSG signal. A high-speed USB/GPIB interface (Keysight 82358B) was used for data-acquisition and to control the LCR-meter in LabVIEW that is on the NI-PXIe 1071 chassis. Measurements for both the RSG and CSGS were collected every 10 seconds. A type-k thermocouple was mounted on the backside of the Al6061 fixture to measure and collect temperature data during the test.

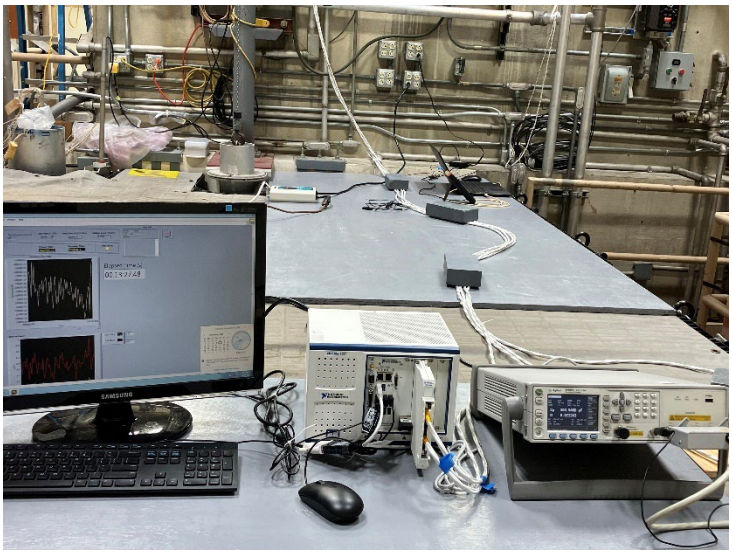

Figure 5. Data acquisition systems used for measuring RSG and CSG signals

2.2.2. Campaign 2

The electrical resistance of the strain gauges was measured using the Keysight data acquisition (DAQ) device (34970A, Keysight) and a LabVIEW program that was used for data acquisition. Sequential collection of multiple RSG were collected using a multiplexer outfitted on the Keyence (DAQM901A, Keysight). Data was collected every 10 seconds to sync up the sampling rate of the OSURR reactor data. The CSG was measured using a precision LCR-meter (Agilent E4980a) using a four-point measuring technique with kelvin clip leads (16089C, Keysight). The CSGs were configured so that sequential measurements of multiple CSGs can be collected using the same Keysight multiplexer on the Keysight DAQ. Data was collected every 10 seconds to sync up the sampling rate of the OSURR reactor data. A type-k thermocouple was mounted on the backside of the Al6061 fixture to measure and collect temperature data during the test.

2.3. Sample Fabrication

For this work, the strain gauges were fabricated using a silver nanoparticle ink (JS-A21AE, Metalon) on an Al6061 substrate with 25 μm (1 mil) thick polyimide tape (Micronova) insulation and encapsulation. AJP was selected as the AM method for fabrication since it can fabricate small form factor devices with a wide variety of ink materials and substrate geometries. The AJP printing process parameters used to print silver are listed in Table 3. The silver strain gauges were sintered at 200 °C for 1 hour in the benchtop muffle furnace (Thermo Scientific Thermolyne) with a heating/cooling rate of 2 °C/min.

Table 3. Silver Ink Printing Parameters

Printing Parameter	Value
Nozzle diameter (μm)	150
Aerosol Jet Atomizer type	Ultrasonic
Carrier/Atomizer gas flow rate (sccm)	27
Sheath gas flow rate (sccm)	57
Number of passes	2
Standoff distance (mm)	3
Platen temperature (°C)	60
Water chiller temperature (°C)	20
Ultrasonic atomizer power (amp)	0.50
Printing speed (mm/s)	4

2.3.1. Campaign 1

In campaign 1, two RSG and two CSG were fabricated. The RSG was designed to utilize two sensors that are fabricated in series (half-bridge RSG). As shown in Figure 6b, the strain sensor is composed of two different gauges: 1) an active gauge that has serpentine electrodes that are parallel to the direction of applied stress and 2) a dummy gauge has serpentine electrodes that are perpendicular with the direction of applied stress. The dummy gauge is oriented so that it is in-sensitive to stress under uniaxial loading and allows for active corrections for errors associated with temperature changes/ fluctuations. The CSG is an interdigitated electrode design (Figure 6a) that are composed of multiple in-plane electrodes that are printed parallel to the substrate [5]. The strain gauges were mounted on a custom Al6061 fixture (Figure 7) and strapped on using aluminum wire to mitigate the interconnection of the wire to the strain gauge from failing when lowering down into the reactor. 40-ft of three wire nickel leads were used to connect to the strain gauges to allow for sufficient length that will reach the bottom of the reactor and to the data acquisition equipment. The wires were bonded to the contact pads of the sensors using a two-part silver epoxy (EPO-TEK H20E, Epoxy Technology, Inc.).

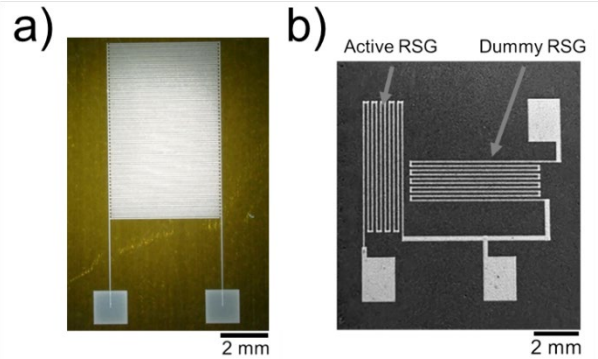

Figure 6. Capacitive strain gauge printed on polyimide insulation and resistive strain gauge printed directly on anodized aluminum surface

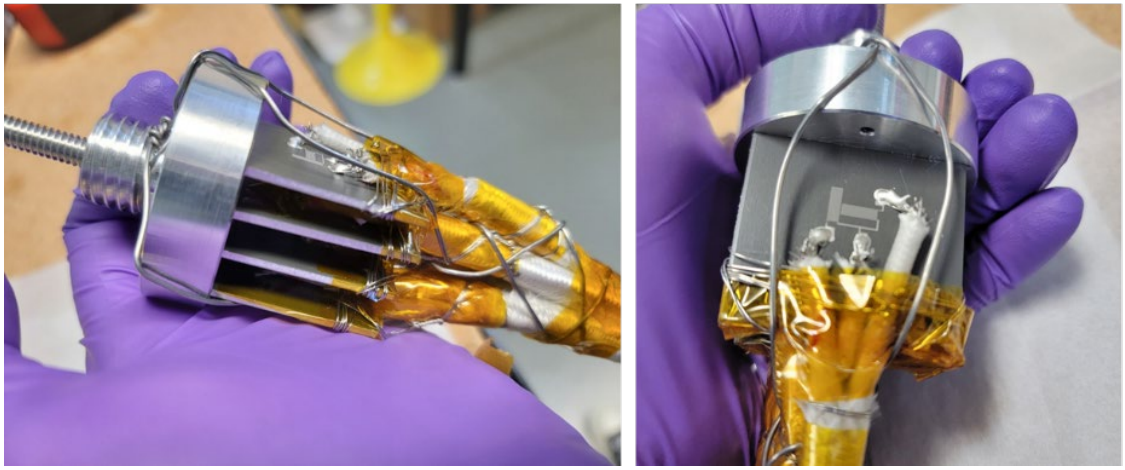

Figure 7. two resistive and two capacitive strain gauges mounted on a fixture to be placed in the furnace and lowered in the 9.5" dry tube. The fixture allowed the position of the strain gauges to be at region where the maximum neutron flux was expected.

2.3.2. Campaign 2

In campaign 2, four RSGs and four CSGs were fabricated on a 35 mm × 10 mm × 0.8 mm (length × width × thickness) Al6061 substrate with a polyimide insulation layer. In the high flux region, an Al6061 fixture was created to accommodate a total of six strain gauges. Two RSGs and two CSGs were pre-strained in a passive mount (Figure 9a) and 1 of each strain gauge was not pre-strained (Figure 9b). Figure 9c shows a representative photo of what the sample looks like when put in the passive mount. Additionally, there were plans to place one RSG and one CSG outside of the furnace as shown in Figure 10b. The strain gauges were mounted on a custom Al6061 fixture (Figure 10b) and additionally strapped on using aluminum wire to mitigate the interconnection of the wire to the strain gauge from failing when lowering down into the reactor. 40-ft of three wire nickel leads were used to connect to the resistive strain gauge to allow for sufficient length that will reach the bottom of the reactor and to the data acquisition equipment. To enable sufficient shielding, the CSGs were connected using a coax mineral insulated copper lead wires during the 2nd campaign. The wires were bonded to the contact pads of the sensors using a two-part silver epoxy (EPO-TEK H20E, Epoxy Technology, Inc.).

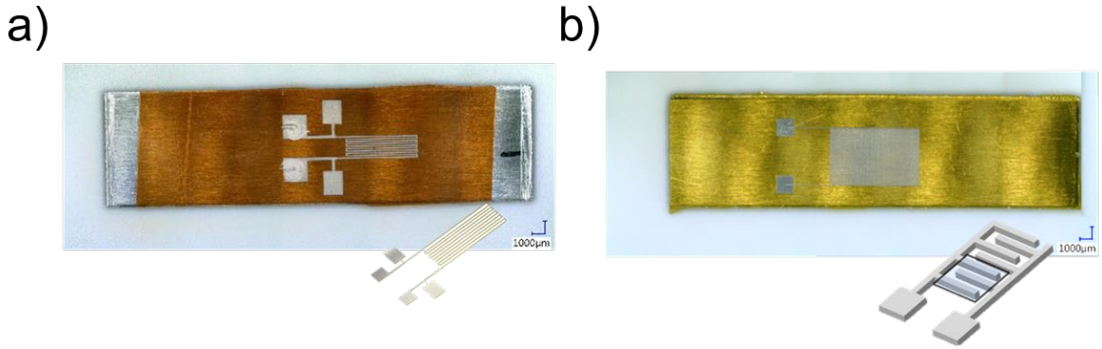

Figure 8. resistance and capacitive strain gauges fabricated on polyimide tape on a 35 × 10 × 0.8 mm (length × width × thickness) Al6061 coupon

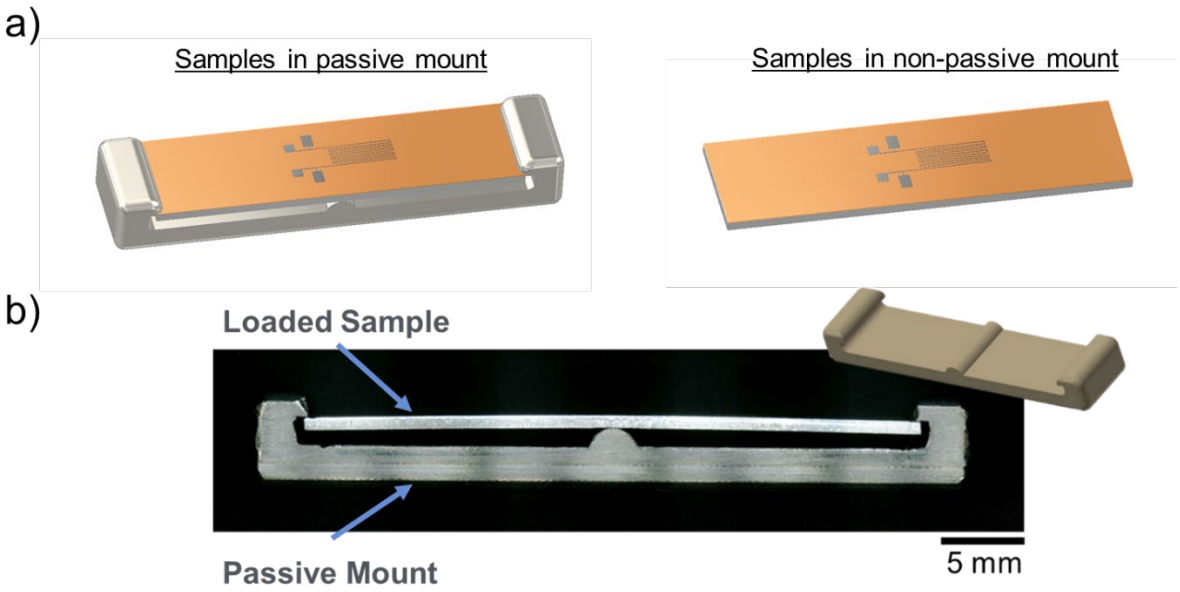

Figure 9. Schematic representation of the Al6061 sample pre-loaded and unloaded in the passive strain 3-point bend mount. b) shows a cross-section of the sample loaded in titanium 3-point bend fixture.

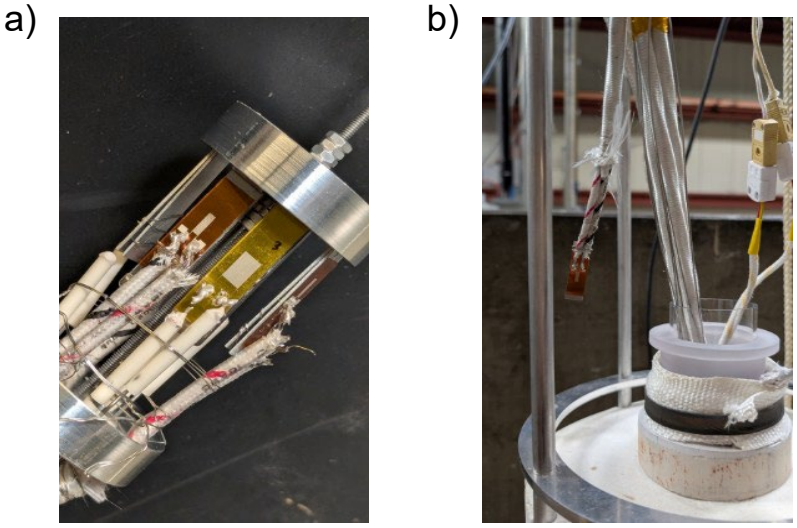

Figure 10. a) Shows the six strain gauges that were loaded in the fixture to allow for the sensing region of the strain gauges to be within the high flux region of OSURR. b) shows a strain gauge secured and placed outside of the furnace.

3. DISCUSSION & RESULTS

3.1. Campaign 1 – Initial test and low neutron flux

Once the furnace was lowered into the dry tube, one of two of the RSGs had sporadic resistance signal indicating that the interconnection may have failed. Additionally, only one of the CSGs were measured during the test due to limitations and concerns with the connections and repeatable. Data acquisition of the CSGs was performed using a single kelvin probe which limits the number of samples that can be tested simultaneously in the 1st campaign. Although the initial intent was to monitor and switch the probing periodically, the manual probing proved to be challenging with inconsistencies with repeatability when switching back and forth. It was decided to just measure one CSG for this initial test.

Figure 11 shows the compiled data of the RSG, CSG, and thermocouple as collected during the four days of testing. Also shown the fluence / cumulative neutron dose accumulation during testing. It can be observed from Figure 11 that there are data spikes in the RSG and CSG results that are a result of noise from the reactor and facilities. In addition, it can be seen that even when the reactor was powered down to 0, overnight data collection showed that both the RSG and CSG still experienced drifting in their signal for all four days.

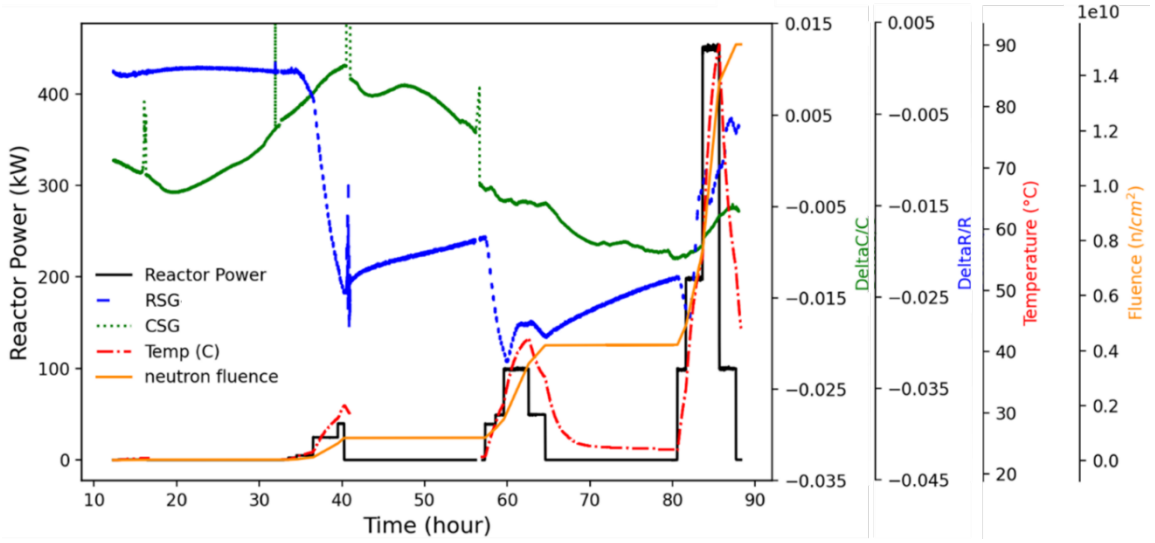

Figure 11. Strain gauge response as a function of time during the four-day irradiation campaign.

Figure 12 separates the response of the four days tested with irradiation and shows the signal of the RSG and CSG during reactor power up, steady-state holds, and reactor power down (

Table 1). It can be seen in Day-1 (Figure 12a) and Day-2 (Figure 12b) of testing that there were spikes in the data. It was found that the RSG and CSGs signals were affected by the noise from both the reactor start-up process, reactor power lines, and reactor coolant pumps. After Day-3 (Figure 12c), the wires were more carefully strapped down to minimize movement and our set-up ending up incorporating a: voltage regulator/isolator, noise filtration device, and use of a common electrical ground to improve the signal noise. These additions mitigated the noise from these extraneous sources and cleaned up the signal. In general, from Figure 12, the CSG had a lower drift and change in signal when compared to the half-bridge RSG. These shifts in signal have implications for causing errors in any potential strain signals that would need to be captured by these sensors. For reference, a change (i.e., $\frac{\Delta R}{R}$ for RSG or $\frac{\Delta C}{C}$ for CSG) of 0.001 - 0.002 of the signal is approximately the expected signal change for a 0.1% (i.e., 1000 με) mechanical strain measurement.

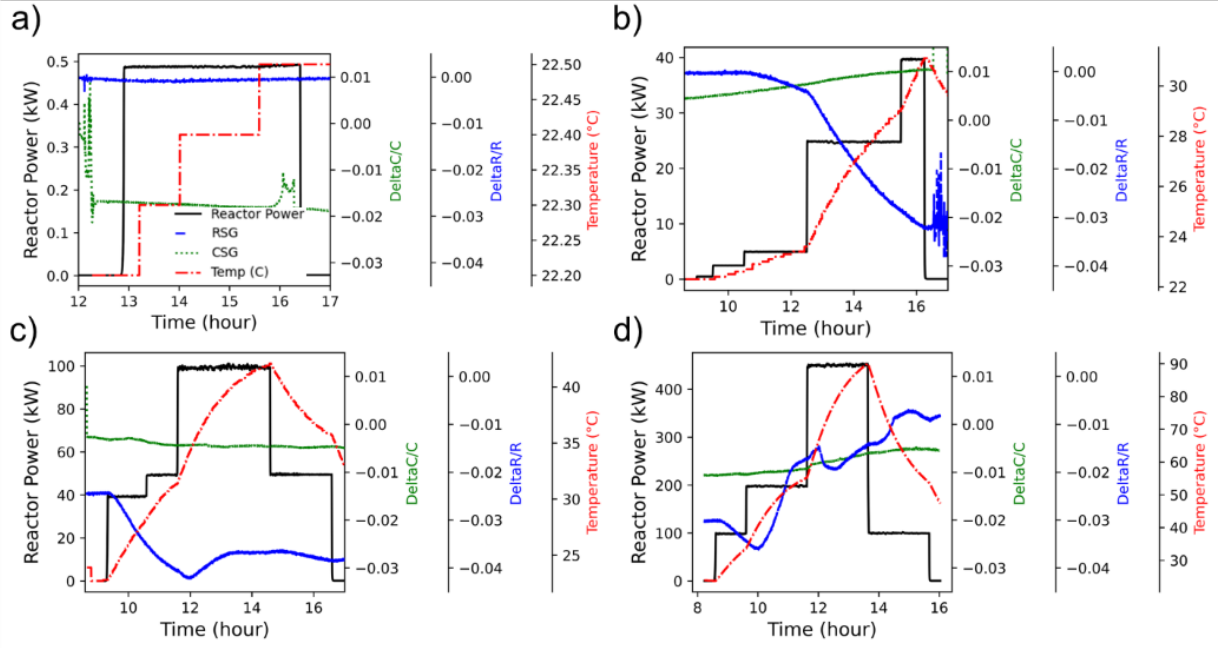

Figure 12. Strain gauge response for day # a) one, b) two, c) three, and d) four.

Figure 13 shows the data from Figure 11 plotted as a function of neutron fluence and shows that the signal from the RSG and CSG had a slight decrease in signal at lower fluence, with a subsequent increase in signal with increase in fluence. It is noted that this increase in signals could also be attributed to the increase in temperature experienced during testing due to gamma heating. This decrease correlates with the decrease in resistivity of silver films at low fluence when irradiated with ions [7]. Vinsek and Carter suggest that the reduction in film resistivity was attributed to the removal of surface contaminants on the film surface. As seen in Figure 13 beyond a flux of $\approx 0.2 \times 10^{10}$ n/cm^2, the subsequent increase in resistivity of silver is expected due to the cumulative concentrations of defects from irradiating the silver with fast and thermal neutron. The total neutron fluence after the 5th day of testing on campaign 1 was approximately 1.5×10^{10} n/cm^2

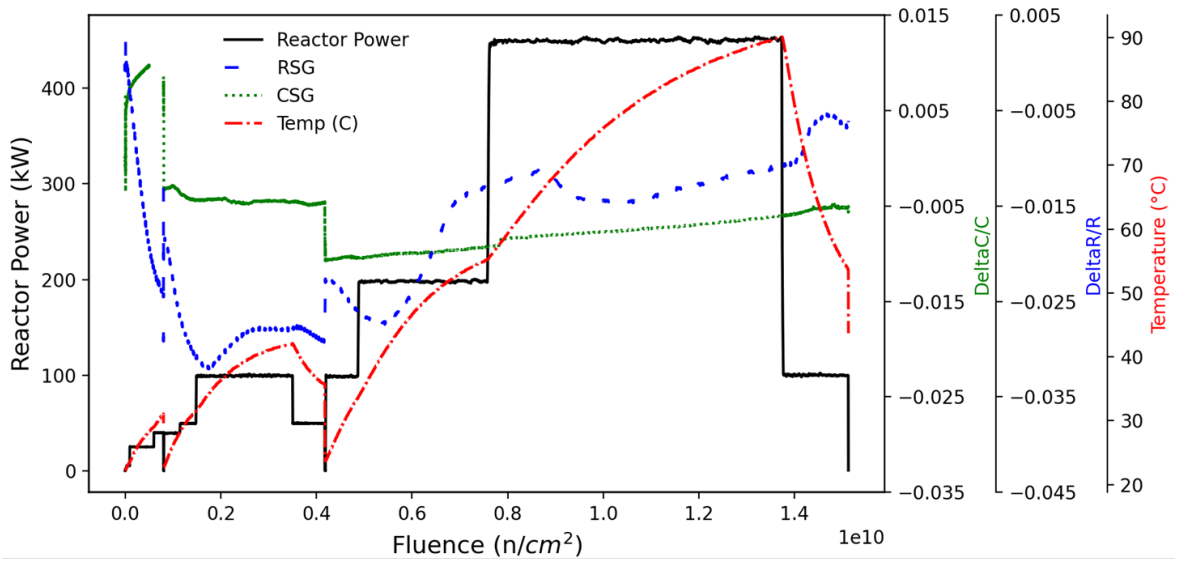

Figure 13. Strain gauge response as a function of fluence/neutron dose

3.2. Campaign 2 – high neutron flux

Prior to testing the reactor with neutron irradiation at OSURR, the response of RSG and CSG with temperature when unloaded and pre-loaded in the passive mount was measured. This test was performed in a lab environment in a muffle furnace and in the reactor with the power at 0 kW and furnace ramped temperature. The results from these two separate tests can be seen in Figure 14. As seen in Figure 14a, when comparing the signal of the strain gauge that was loaded and the strain gauge not loaded, the signal response was slower during both the heat-up and cool-down the one that was preloaded with the titanium fixture. Heating the sample up with the addition titanium passive mount fixture slows down the response due to the added mass and the lower thermal conductivity. The coefficient of thermal expansion (CTE) and thermal conductivity of the titanium fixture is 8.6 µm/m·K and 21.9 W/m-K, respectively. The CTE and thermal conductivity of the Al6061 couple is 23.6 µm/m·K and 167 W/m-K, respectively. The strain gauges return back to the original value after the thermal cycle up to 200 °C. Also observed is that the sensitivity and response (i.e., thermal coefficient of resistance) of the strain gauges were different despite being the same material and features.

During transportation and lowering the samples into the reactor, a total of three RSGs survived with the remainder of the samples failing at the junction between the lead wire and strain gauge contact pads. There are plans to perform post-irradiation examination (PIE) of these strain gauges and their components. As a result, Figure 15 shows the results of three RSGs which were oriented in the following configuration:

1) RSG-1: not in passive mount in the high flux region of the furnace
2) RSG-2: pre-strained in the passive mount in the high neutron flux region of the furnace
3) RSG-3: not in passive mount outside of the furnace in a region with negligible neutrons and gamma irradiation

Figure 14b shows the response of the three resistive strain gauges testing at the OSURR on the first day where the reactor power was kept off and the furnace was utilized. The signal sensitivity of RSG-1 and RSG-2, which were placed in the furnace, to temperature are different which is similar to the results during the furnace testing. However, after a full thermal cycle the signal of RSG-1 and RSG-2 do not return to its original value which shows hysteresis within the signal. RSG-3 showed little to no change caused by the furnace since it was placed outside of the furnace (Figure 10).

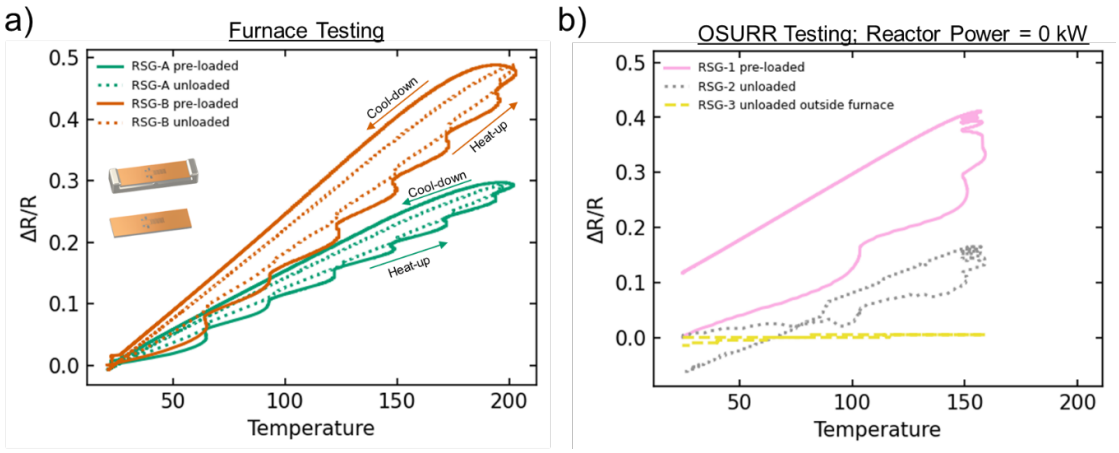

Figure 14. Response of the resistive strain gauge in a furnace while pre-loaded and unloaded in the titanium passive 3-point bend mount up to 200 °C. The response of the strain gauges on the first day at the Ohio State University Research Reactor with reactor at 0 kW and furnace turned on to heat the sample up to 150 °C.

The signals from RSG-1, RSG-2, and RSG-3 as a function of neutron fluence (as calculated at the maximum flux region) are shown in Figure 15. The signal of RSG-1 increased substantially faster than RSG-2 after the first initial day (i.e., Day-2) of irradiation at 225 kW reactor power. After the first day of irradiation, the RSG signal of RSG -1 does not return back to its original state and eventually experienced an open circuit. The signal from RSG-1 remained in this degraded/failed state for the remainder of the experiment. The signals from both RSG-2 and RSG-3, however, showed a slight increase in its signal (relative to RSG-1) and returns back to their original state after days 2 and day 3 of testing. On day-4 of testing, in addition to a reactor power of 450 kW the furnace was utilized to incorporate two thermal cycles up to ≈ 215 °C (Table 2). After the second external temperature ramp cycle up to ≈ 215 °C, the signal of RSG-2 temporarily loses signal. This was suspected to be caused by failure of the interconnection bond at the wire / strain gauge. The RSG-2 signal subsequently came back to its original reading upon cool-down. During day-5 of testing, RSG-2 did not experience the same large fluctuation despite the ramping the temperature up to 215 °C again and holding for 1 hr. The signal from RSG-3 remained relatively flat compared to RSG-1 and RSG-2. The slight increase from RSG-3 could be from residual radiation/convective heat from the furnace due to its proximity to the outlet of the furnace (Figure 10) and/or damage from the low neutron/gamma flux in this area. The total neutron fluence after the 5th day of testing on campaign 1 was approximately 1.3×10^{17} n/cm^2.

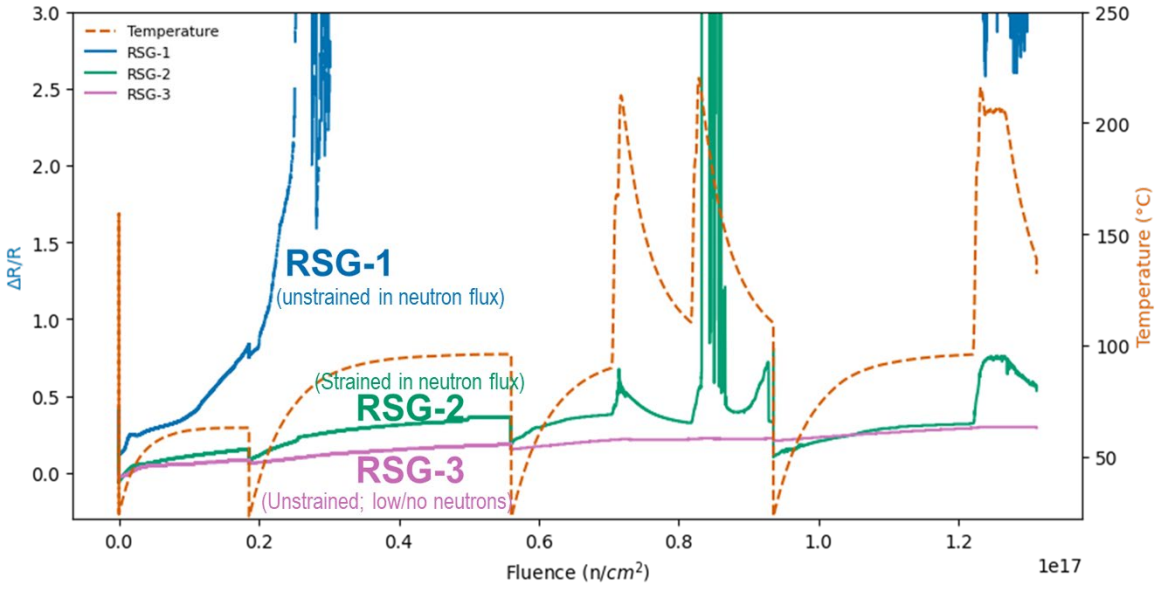

Figure 15. Signal of the resistive strain gauge as a function of neutron fluence, as calculated at the peak neutron flux region of the reactor in the 9.5" dry tube.

Figure 16 shows the response of RSG-1, RSG-2, and RSG-3 as a function of temperature caused by gamma heating and external heating from the furnace during the 5-day test for campaign 2. The signal from RSG-1 increased and saw degradation in the signal almost immediately during testing. There was significant hysteresis of the signal. The signal from RSG-2 was relatively linear with little hysteresis, however showed degradation above 150 °C. This was also seen in Figure 15. The signal, however, returned during cool-down and remained connected for irradiation on Day-5. The signal for RSG-3 remained relatively stable and unchanged.

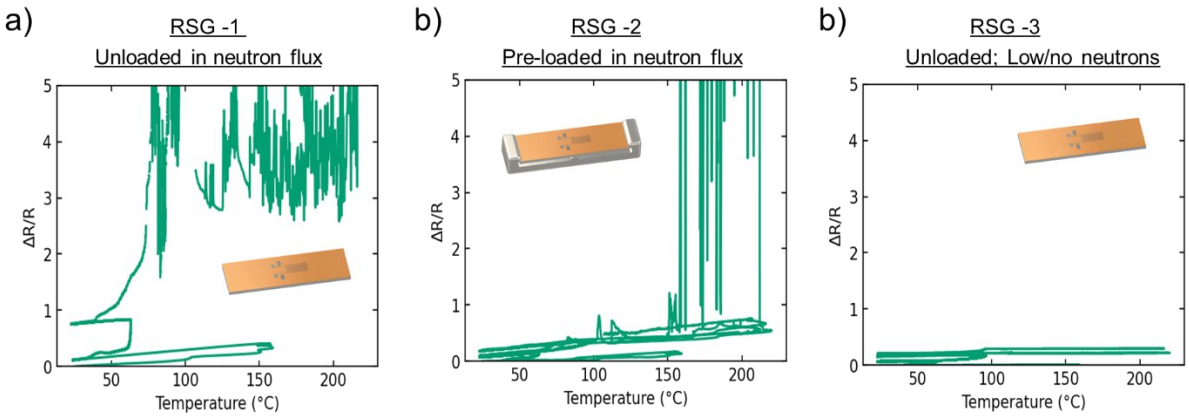

Figure 16. Response of RSG-1, RSG-2, RSG-3 as a function of temperature in the furnace due to gamma heating and external heating from the heating elements of the furnace.

4. CONCLUSION

In campaign 1, the printed capacitive and resistive strain gauges were gradually exposed to neutron irradiation at the Ohio State University Research Reactor. This allowed for a total neutron fluence of 1.5 $\times 10^{10}$ n/cm^2. at the peak flux region in the 9.5" dry tube. It was observed that the signals were attenuative

to noise from both the reactor start-up process, reactor power lines, and reactor coolant pumps that caused error in the signal. After carefully strapping the wires down to minimize movement and incorporating 1) voltage regulator/isolator, noise filtration device, and using a common electrical ground, it was found that the signal noise was mitigated from these extraneous sources. In general, the capacitive strain gauge had a lower drift in its signal when compared to the half-bridge resistive strain gauge. These shifts in signal have implications for causing errors in any potential strain signals that would need to be captured by these strain gauges.

In campaign 2, the signal noise was mitigated with the lessons learned from the 1st campaign, and a switch was used to enable read-out from multiple resistive and capacitive strain gauges simultaneously. The strain gauges were exposed to the maximum reactor power for longer allowing for a total neutron fluence of 1.3×10^{17} n/cm^2. at the peak flux region in the 9.5" dry tube. Temperature was observed to be a dominant factor affecting the signal of the resistive strain gauge. Neutron and gamma irradiation damage could be a contributing factor to hysteresis and loss of signal. PIE will be performed on the strain gauges to investigate the extent of degradation and damage to the AM strain gauges after neutron exposure.

5. REFERENCES

[1] D. Knudson and J. Rempe, "Evaluation of LVDTs for use in ATR irradiation experiments," Idaho National Laboratory (INL), 2009.

[2] M. T. Rahman, R. Moser, H. M. Zbib, C. V. Ramana, and R. Panat, "3D printed high performance strain sensors for high temperature applications," (in English), *J Appl Phys,* vol. 123, no. 2, pp. 1-12, Jan 14 2018, doi: Artn 024501 10.1063/1.4999076.

[3] L. M. Faller, W. Granig, M. Krivec, A. Abram, and H. Zangl, "Rapid prototyping of force/pressure sensors using 3D-and inkjet-printing," (in English), *J Micromech Microeng,* vol. 28, no. 10, Oct 2018, doi: ARTN 104002 10.1088/1361-6439/aaadf4.

[4] T. L. Phero, A. R. Khanolkar, and M. D. McMurtrey, "Printed Strain Gauges for High Temperature Applications (> 300 C)," Idaho National Laboratory (INL), Idaho Falls, ID (United States), 2023.

[5] T. L. Phero, K. A. Novich, B. C. Johnson, M. D. McMurtrey, D. Estrada, and B. J. Jaques, "Additively manufactured strain sensors for in-pile applications," *Sensors and Actuators A: Physical,* vol. 344, p. 113691, 2022.

[6] T. O. S. U. C. o. Engineering. "Nuclear Reactor Laboratory - Research Reactor." https://reactor.osu.edu/facilities/research-reactor (accessed December 18, 2024).

[7] B. Navinsek and G. Carter, "Electrical resistivity changes in thin metallic films due to ion irradiation," *Applied Physics Letters,* vol. 10, no. 3, pp. 91-92, 1967.